EPR and optical-absorption studies of Cu2+-doped Zn(NH2(CH2)3NHOH)2Ni(CN)4 single crystals

5 AUTHORS, INCLUDING:

Recep Tapramaz
Ondokuz Mayıs Üniversitesi
21 PUBLICATIONS **237** CITATIONS

EPR and Optical-Absorption Studies of Cu²⁺-Doped Zn(NH₂(CH₂)₃NHOH)₂Ni(CN)₄ Single Crystals

H. Paşaoğlu[1], **B. Karabulut**[1], **G. Kaştaş**[1], **R. Tapramaz**[1], and **A. Karadağ**[2]

[1] Department of Physics, Faculty of Art and Sciences, Ondokuz Mayıs University, Samsun, Turkey
[2] Department of Chemistry, Faculty of Sciences, Gazi Osmanpasa University, Tokat, Turkey

Abstract. Electron paramagnetic resonance of Cu²⁺-doped catena-*trans*-bis(N-(2-hydroxyethyl)-ethylenediamine) zinc(II)-tetra-μ-cyanonicelate(II) [Zn(NH₂(CH₂)₃NHOH)₂Ni(CN)₄] single crystals and powder are examined at room temperature. The spectra show the substitution of the Zn²⁺ ion with the Cu²⁺ ion. The crystal field around the Cu²⁺ ion is nearly axial. There is a single paramagnetic site with $g_{xx} = 2.073$, $g_{yy} = 2.060$, $g_{zz} = 2.248$, $A_{xx} = 40.5$ G, $A_{yy} = 50.8$ G, $A_{zz} = 172.0$ G. The ground-state wave function is an admixture of $d_{x^2-y^2}$ and d_{z^2} states. The optical-absorption studies show two bands at 320 nm (31250 cm⁻¹) and 614 nm (16286 cm⁻¹), which confirm the axial symmetry. The crystal field parameters and the wave function are determined.

1 Introduction

It is well known that the transition-metal ions as a probe can be used to determine the symmetry of the environment of complexes in the host lattices by the electron paramagnetic resonance (EPR) technique. The EPR spectra of the Cu²⁺ ion have been studied extensively and found to be informative about the environmental effects [1–7]. In the Cu²⁺-doped compounds, the Cu²⁺ ion replaces the divalent cation present in the lattice, whereas there are some studies reporting that Cu²⁺ ions replace the monovalent cation in the host lattice substitutionally.

Cyanocomplexes are popular in coordination and organometallic chemistry. Recently, cyanocomplexes possessing various degrees of dimensionality and containing paramagnetic central atoms have often been the subject of magnetic studies. The ability of the cyano group to link various atoms is used in the field of supramolecular chemistry to build one-, two- and three-dimensional structures [8]. In this case, in addition to their structural function, cyanocomplex anions also exhibit an important magnetic and electronic function. For this reason, various physical phenomena related with magnetism can be investigated by means of these complexes [9–11].
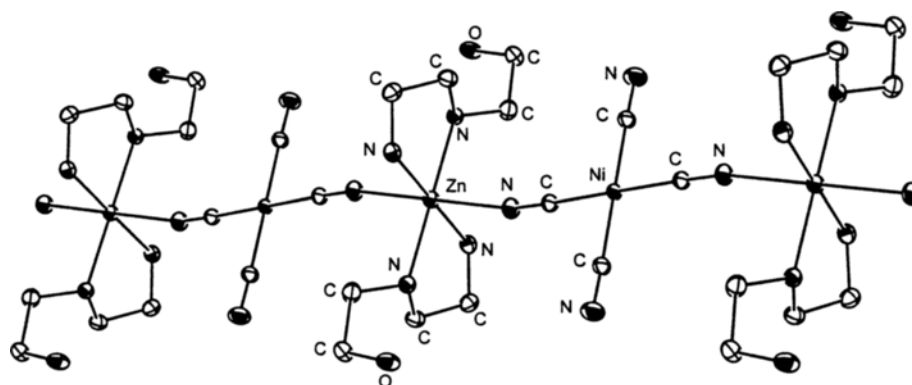
Fig. 1. Structure of the Zn(hydet-en)$_2$Ni(CN)$_4$ complex. The Cu^{2+} ion substitutes the Zn^{2+} ion in the complex.

Single-crystal X-ray studies of the Zn(NH$_2$(CH$_2$)$_3$NHOH)$_2$Ni(CN)$_4$ complex show that the asymmetric unit cell consists of one *trans*-[Zn(hydet-en)$_2$]$^{2+}$ cation (where hydet-en is NH$_2$(CH$_2$)$_3$NHOH) and one *trans*-[Ni(CN)$_4$]$^{2-}$ anion with the inversion center located at the Zn atom (Fig. 1). Each Zn^{2+} ion is in the octahedral coordination through two nitrogen atoms of the cyanide bridge and nitrogen donors of hydet-en ligands. Therefore, it is of interest to investigate the EPR spectra of Cu^{2+}-doped Zn(hydet-en)$_2$Ni(CN)$_4$ single-crystal and powder samples with the aim to provide a detailed description of the paramagnetic center, the electrical field symmetry produced by the ligands around the metal ion, the nature of the bonding of the metal ion with different ligands, and optical d-d transitions.

2 Experimental

60 cm^3 of an ethanol solution of ZnCl$_2$ (1 mmol, 0.136 g) was added to 40 cm^3 of an aqueous solution of K$_2$[Ni(CN)$_4$]·2H$_2$O (1 mmol, 0.241 g). The cream precipitate is formed after approximately 5 min of stirring. It is then dissolved in a bulb containing 0.210 g (2 mmol) of N-(2-hydroxyethyl)-ethylenediamine. The resultant light-yellow solution is filtered for any present solid impurities. Finally, a very small amount of CuSO$_4$·5H$_2$O is added to the solution as impurity and the solution is left to crystallize. Well-developed single crystals are obtained after about one week.

Zn(hydet-en)$_2$Ni(CN)$_4$ is of triclinic symmetry with the space group P_{-1} and contains one molecule in a unit cell. The unit cell dimensions are $a = 0.7222$ nm, $b = 0.7900$ nm, $c = 0.9048$ nm and the angles are $\alpha = 99.25°$, $\beta = 101.71°$ and $\gamma = 105.99°$ [12].

A Varian E-109 C Model X-band EPR spectrometer is used to record the spectra with a magnetic field modulation frequency of 100 kHz. The single crystal

is mounted on a goniometer and the spectra were recorded in three perpendicular planes (a^*c^*, a^*b, bc^*) with 10° intervals at room temperature. Diphenyl-picrylhydrazil sample ($g = 2.0036$) is used to determine the g-value.

Optical absorption spectra of the Zn(hydet-en)$_2$Ni(CN)$_4$ single crystals are recorded at room temperature on a CINTRA 20 UV-VIS spectrometer with diffuse reflectance accessory working in the interval from 300 to 900 nm.

3 Results and Discussion

The EPR spectra of the Cu^{2+}-doped Zn(hydet-en)$_2$Ni(CN)$_4$ single crystal recorded in three perpendicular planes at room temperature show only one set of four lines, which is attributed to the Cu^{2+} ion. Figure 2 shows the EPR spectrum of Cu^{2+}-doped Zn(hydet-en)$_2$Ni(CN)$_4$ single crystals in the bc^* plane with magnetic field 50° and 60° away from the c^* axis. The spectrum is compatible with the triclinic symmetry of the Zn(hydet-en)$_2$Ni(CN)$_4$ single crystal. Since the line width is relatively large, the naturally abundant ^{63}Cu and ^{65}Cu lines are not clearly resolvable in all orientations. Angular variations show the presence of only one magnetic site for the Cu^{2+} ion in the single crystal as shown in Fig. 3.

The $g^2(\theta)$ and $A^2(\theta)$ hyperfine values of all lines are plotted against the rotation angle in three planes and they are fitted to Eq. (1) to obtain $\mathbf{g}^2$ and $\mathbf{A}^2$ tensor elements
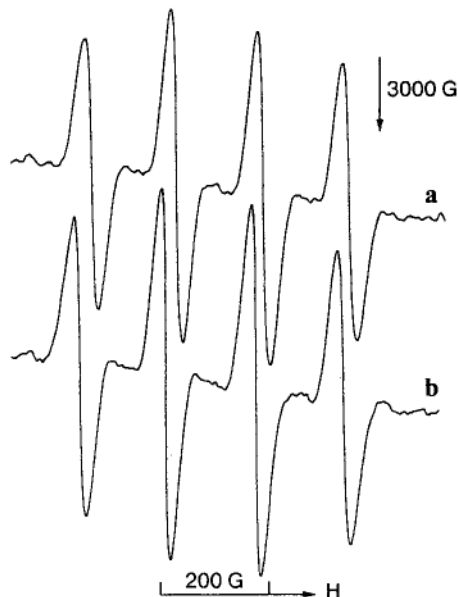

Fig. 2. EPR spectrum of the Cu^{2+}-doped Zn(hydet-en)$_2$Ni(CN)$_4$ single crystal for two crystal orientations. The magnetic field is in the bc^* plane and is 50° (a) and 60° (b) away from the c^* axis.
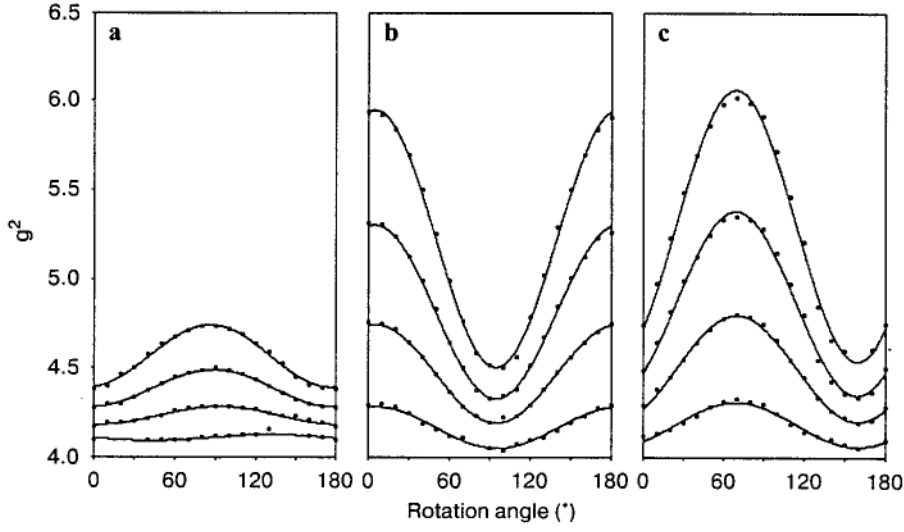
Fig. 3. Angular variations of the g^2 values of all lines in three mutually perpendicular planes a^*c^* (a), ba^* (b), and c^*b (c) of the Cu^{2+}-doped Zn(hydet-en)$_2$Ni(CN)$_4$ single crystal.

$$g_k^2(\theta) = g_{ii}^2 \cos^2\theta_i + g_{jj}^2 \sin^2\theta_j + 2g_{ij}^2 \sin\theta_i \cos\theta_j,$$
$$A_k^2(\theta) = a_{ii}^2 \cos^2\theta_i + a_{jj}^2 \sin^2\theta_j + 2a_{ij}^2 \sin\theta_i \cos\theta_j, \qquad (1)$$

where $i, j, k \equiv x, y, z$.

The spectra can be described in terms of a spin Hamiltonian of the form

$$\mathcal{H} = \beta B g S + S A I, \qquad (2)$$

which includes only electronic Zeeman and hyperfine interactions with nuclear Zeeman and quadrupole interactions neglected. In order to find the g and hyperfine values, we have used an iterative numerical technique described in ref. 13. **g** and **A** tensors are constructed and diagonalized to find principal values

Table 1. Principal values of **g** and **A** tensors of Cu^{2+} doped in Zn(hydet-en)$_2$Ni(CN)$_4$ single crystals at room temperature ($\Delta g = \pm 0.002$, $\Delta A = \pm 5$ G).

g	Direction cosines			A (G)	Direction cosines		
	a^*	b	c^*		a^*	b	c^*
$g_{xx} = 2.073$	−0.923	−0.333	0.191	$A_{xx} = 40.5$	−0.982	−0.135	0.125
$g_{yy} = 2.059$	−0.377	0.877	−0.296	$A_{yy} = 50.8$	−0.116	0.927	−0.331
$g_{zz} = 2.248$	0.067	0.345	0.935	$A_{zz} = 172.0$	0.071	0.347	0.935

Table 2. Spin Hamiltonian parameters for Cu^{2+}-doped $Zn(hydet-en)_2Ni(CN)_4$ single crystals and other related systems ($\Delta g = \pm 0.002$, $\Delta A = \pm 5$ G).

Lattice	$g_\parallel$	$g_\perp$	$A_\parallel$ (G)	$A_\perp$ (G)	Reference
$Zn(hydet-en)_2Ni(CN)_4$	2.248	2.066	172.0	46.2	Present work
Cadmium(II) formate dihydrate	2.274	2.094	251.5	153.0	1
L-Alanine	2.261	2.056	187.0	32.5	15
α-Glycine	2.236	2.059	135.0	15.5	15
2-Methylalanine	2.204	2.048	152.5	19.0	15
$Cu(II)/Zn(Im)_6Cl_2 \cdot 4H_2O$	2.313	2.104	146.6	38.2	18
$Cu/ZnNi(CN)_4$/Species B	2.332	2.082	142.6	33.0	14
LiBaB	2.284	2.053	122.9	26.1	29
NaBaB	2.262	2.049	129.9	25.1	29
KBaB	2.259	2.048	132.8	25.1	29
$Cd(CH_3NH_2CH_2COO)Cl_2$	2.213	2.052	183.0	30.8	30
$Zn(hydet-en)_2Ni(CN)_4$ powder	2.245	2.061	170.7	46.0	Present work

and are found to be nearly axially symmetric. The results are given in Table 1. Since the direction cosines of principal g and hyperfine values are nearly coincident, they are to have the same orientation in the crystal (Table 1). The principal values of these tensors and some other values reported earlier are given in Table 2, where $g_\perp = (g_{xx} + g_{yy})/2$, $g_\parallel = g_{zz}$, $A_\perp = (A_{xx} + A_{yy})/2$ and $A_\parallel = A_{zz}$ [14–18].

Figure 4 shows the powder EPR spectrum of Cu^{2+}-doped $Zn(hydet-en)_2Ni(CN)_4$. Since the powder spectrum is very weak, we increased the modulation and power to the order of the line width (40 G) and 3 dB, respectively. As expected, this arrangement distorted the spectrum; therefore, the perpendicular components of

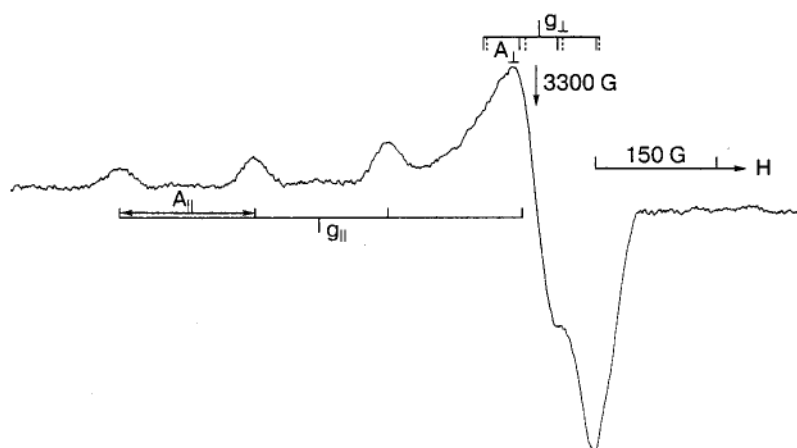

Fig. 4. Powder spectrum of the Cu^{2+}-doped $Zn(hydet-en)_2Ni(CN)_4$ complex. The stick diagram in the perpendicular part (solid line) shows the second-order interactions and the dashed lines show normal hyperfine lines. $\nu = 9.52$ GHz.

Table 3. Molecular orbital coefficients of Cu^{2+}-doped $Zn(hydet-en)_2Ni(CN)_4$ single crystals at room temperature. Some other results of related system are also included for comparison.

Lattice	γ^2	β_1^2	$(g_e - g_{\parallel})/(g_e - g_{\perp})$	Reference
$Zn(hydet-en)_2Ni(CN)_4$	0.70	0.86	3.8	Present work
$Zn(hydet-en)_2Ni(CN)_4$ powder	0.70	0.86	4.1	Present work
Cadmium(II) formate dihydrate	1.00	0.63	2.9	1
$Cu/ZnNi(CN)_4$	0.99	0.76	4.1	14
LiBaB	0.65	0.81	5.5	29
NaBaB	0.65	0.74	5.5	29
KBa B	0.65	0.73	5.6	29
$Cd(CH_3NH_2CH_2COO)Cl_2$	0.94	0.79	4.2	30

the powder spectrum do not show all the details seen in the spectrum. Second-order corrections of the $A_{\perp}$ value is included in Fig. 4. The EPR data from the powder give almost the same values as single crystals (Table 2).

The observed nearly axial symmetry of the **g** and **A** tensors can be explained in terms of the slightly distorted octahedral coordination around the Cu^{2+} ion. An octahedral complex with a tetragonal elongation would give $g_{\parallel} > g_{\perp} > g_e$ and the tetragonality measure $|(g_e - g_{\parallel})/(g_e - g_{\perp})|$ is given in Table 3.

The Cu^{2+} ions substitute Zn^{2+} in the host lattice. The ionic radius of Zn^{2+} (75 pm) is enough for the substitution with Cu^{2+} (72 pm). The Cu^{2+} ion forms an octahedral complex with two of the ligands being two bridging cyanide-nitrogen atoms and the other four planar ligands being four nitrogen atoms of the two hydet-en groups. Two cyanide-nitrogens in the *trans* position coordinate to the adjacent Ni ions. Ni atoms form the inversion center of the linear chain and the slightly distorted octahedral Cu^{2+} complex lies on the twofold rotation axis.

The ground-state wave function of the Cu^{2+} ion with the d^9 configuration in the octahedral symmetry is determined by several authors [19–23], and the same method is used in this work. The behavior of the hyperfine and g-value variations show that the octahedron is slightly distorted to the tetragonal symmetry via the degenerate $d_{x^2-y^2}$ orbital. The ^2D state of the Cu^{2+} ion in the octahedral crystal field splits into a triplet T_g and a doublet E_g state. Depending on the slight distortion of the octahedron, the E_g state changes to $d_{3z^2-r^2}$ or to $d_{x^2-y^2}$. But when the symmetry gets lower, the ground state is neither $d_{3z^2-r^2}$ nor $d_{x^2-y^2}$, instead, it is a mixture of both. Therefore the ground-state wave function of the Cu^{2+} ion should be a linear combination of $d_{x^2-y^2}$ and $d_{3z^2-r^2}$ orbitals and it can be written as

$$\psi = \alpha'(\alpha|x^2 - y^2\rangle + \beta|3z^2 - r^2\rangle),\tag{3}$$

where α' is the covalency parameter and its square is the probability of finding the electron in the metal d orbitals. The normalization condition for mixing coefficients α and β is
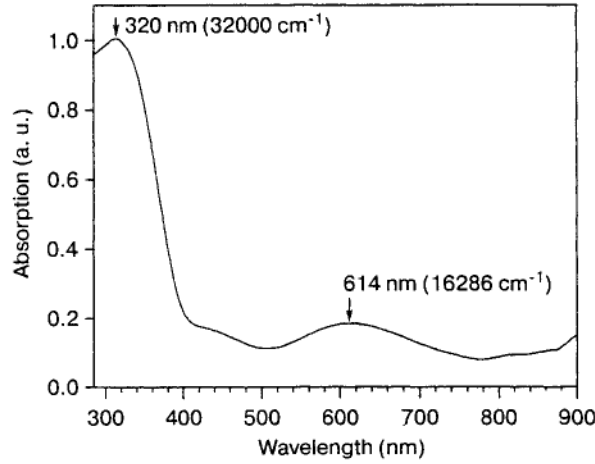
Fig. 5. Optical-absorption spectrum of the Cu²⁺-doped Zn(hydet-en)₂Ni(CN)₄ single crystal.

$$\alpha^2 + \beta^2 = 1. \tag{4}$$

With the experimental values for the Zn(hydet-en)₂Ni(CN)₄ single crystal, the ground-state wave function can be constructed as

$$\psi = (0.903)^{1/2} \left(0.991 \left| x^2 - y^2 \right\rangle + 0.131 \left| 3z^2 - r^2 \right\rangle \right). \tag{5}$$

From these results, the value of $\alpha'^2 = 0.903$ obviously explains that the unpaired electron spends approximately 10% of its time on ligand orbitals, whereas the rest is spent on the Cu²⁺ d orbitals [20].

The room temperature optical-absorption spectrum of the Cu²⁺-doped Zn(hydet-en)₂Ni(CN)₄ single crystal in the 300–900 nm interval is shown in Fig. 5. There are two bands in the visible range at 320 nm (31250 cm⁻¹) and 614 nm (16286 cm⁻¹). The broad band is assigned to the ($^2B_{1g} \rightarrow {}^2B_{2g}$) $d_{xy} \leftrightarrow d_{x^2-y^2}$ transition of the Cu²⁺ ion in the distorted octahedral site. The other band is assigned to the charge transfer band between the metal ion and ligands. Metal–ligand charge transfer mainly occurs in unoccupied π^* orbitals of such ligands as CO, CN and SCN [23]. By correlating EPR and optical absorption data, the molecular orbital coefficients γ^2 and β_1^2 are expressed by using the formulas given in the literature [23–26] as follows,

$$\gamma^2 = \frac{7}{4} \left(\frac{A_{\parallel}}{P} - \frac{A}{P} + \frac{2}{3} g_{\parallel} - \frac{5}{21} g_{\perp} - \frac{6}{7} \right), \tag{6}$$

$$g_{\parallel} = 2.0023 \left[1 - \frac{4\lambda \gamma^2 \beta_1^2}{E_1} \right], \tag{7}$$

where $A = (A_\parallel + A_\perp)/3$, E_t is the energy corresponding to the $^2B_{1g} \rightarrow {}^2B_{2g}$ transition, P is a constant (0.036 cm^{-1}), λ is the spin-orbit coupling constant (-828 cm^{-1} for the Cu^{2+} ion) and g_e is the free electron g-value, ($g_e = 2.0023$). The parameters γ^2 and β_1^2 can be taken as a measure of the in-plane σ bonding and in-plane π bonding between the d orbital of the central metal ion and p orbitals of the ligands [27–29]. Using the above equations, the values of γ^2 and β_1^2 are calculated. The values are given in Table 3. The results of some other works are also included for comparison.

Both γ^2 and β_1^2 are smaller than unity and they indicate the covalent or ionic character of bonding between metal and ligand orbitals. If their values are in the order $\beta_1^2 < \gamma^2$, the in-plane π bonding is more covalent than the in-plane σ bonding, otherwise σ bonding is more covalent and the π bonding becomes significantly ionic [1, 14, 24, 29, 30]. Table 3 shows that the molecular orbital coefficients obtained by correlating EPR and optical data indicate that the in-plane σ bonding is more covalent, whereas the in-plane π bonding is more ionic.

4 Conclusions

The EPR and optical absorbtion spectra of the Cu^{2+}-doped Zn(hydet-en)$_2$Ni(CN)$_4$ single crystal and powder are investigated. The angular variation of single-crystal EPR spectra shows the presence of only one paramagnetic impurity site. The Cu^{2+} ion substitutes the Zn^{2+} ion in the host lattice. The principal g and hyperfine values of the Cu^{2+} complex are evaluated. Both values possess nearly axial symmetry. The detailed study shows that the octahedral site occupied by the Cu^{2+} ion is slightly distorted to tetragonal symmetry (Tables 1 and 3). The ground-state wave function coefficients obtained from spectral data indicate the mixing of $d_{x^2-y^2}$ and $d_{3z^2-r^2}$ orbitals. The molecular orbital coefficients β_1^2 and γ^2 are evaluated. These values indicate that the in-plane π bonding is significantly ionic and the in-plane σ bonding is nearly covalent.

References

1. Kirpal R., Misra S.: J. Phys. Chem. Solids **65**, 939 (2003)
2. Satyanarayana N.: J. Phys. Chem. Solids **47**, 55 (1986)
3. Gopal N.O., Narasimhulu K.V., Rao J.L.: Physica B **307**, 117 (2001)
4. Korkmaz M., Aktaş B.: J. Phys. Chem. Solids **45**, 259 (1984)
5. Venkateshwarlu M., Rao T.B.: Solid State Commun. **82**, 837 (1992)
6. Narasimhulu K.V., Sunandana C.S., Rao J.L.: J. Phys. Chem. Solids **61**, 1209 (2000)
7. Chand P., Umar M.: Phys. Status Solidi B **127**, 279 (1985)
8. Černák J., Orendáč M., Potočňák I., Chomič J., Orendáčová A., Skoršepa J., Feher A.: Coord. Chem. Rev. **224** 51 (2002)
9. Sopkova A., Singliar M. in: The Sorptive Abilities of Tetracyanocomplexes, Inclusion Compound (Atwood J.L., Davides J.E.D., MacNicol D.D., eds.), Vol. 3. New York: Academic Press 1984.
10. Dagotto E.: Phys. World **1996** 22.
11. Orendac M., Orendacova A., Cernák J., Feher A., Signore P.J.C., Meisel M.W., Merah S., Verdaguer M.: Phys. Rev. B **52**, 3535 (1995)
12. Karadağ A., Pasaoglu H., Kastas G., Büyükgüngör O.: Z. Kristallogr. **220**, 74–78 (2005)

13. Karabulut B., Tapramaz R.: Radiat. Phys. Chem. **55**, 331–335 (1999)
14. Murugesan R., Subramanian S.: J. Magn. Reson. **36**, 399 (1979)
15. Fujimato M., Janecka J.: J. Chem. Phys. **55**, 1152 (1971)
16. Anthonisamy V.S.X., Anantharam R., Murugesan R.: Spectrochim. Acta A **55**, 135 (1999)
17. Murugesan R., Subramanian S.: Mol. Phys. **52**, 129 (1984)
18. Rao P.S., Subramanian S.: J. Magn. Reson. **22**, 191 (1976)
19. Tapramaz R., Karabulut B., Köksal F.: J. Phys. Chem. Solids **61**, 1367 (2000)
20. Rao T.B., Narayana M.: Phys. Status Solidi B **106**, 601–606 (1981)
21. Bleaney B., Bower K.D., Price M.H.L.: Proc. R. Soc. Lond. A **228**, 166 (1955)
22. Sroubek Z., Zdansky K.: J. Chem. Phys. **44**, 3078 (1966)
23. Zhan S., Guo D., Zhang X., Du C., Zhu Y., R. Yang: Inorg. Chim. Acta **298**, 57 (2000)
24. Rao J.L., Sivaramaiah G., Gopal N.O.: Physica B **349**, 206–213 (2004)
25. Rao A.S., Rao J.L., Lakshman S.V.J.: J. Phys. Chem. Solids **53**, 1221 (1992)
26. Kivelson D., Neimann R.: J. Chem. Phys. **35**, 149 (1961)
27. Kuska H.A., Rogers M.T., Drullinger R.E.: J. Phys. Chem. **71**, 109 (1967)
28. Imagawa H.: Phys. Status Solidi **30**, 469 (1968)
29. Sreekanth Chakradhar R.P., Murali A., Lakshmana Rao J.: J. Alloys Compd. **265**, 29 (1998)
30. Padiyan D.P., Muthukrishnan C., Murugesan R.: J. Magn. Magn. Mater. **222**, 251 (2000)

Authors' address: Bunyamin Karabulut, Ondokuz Mayıs University, Faculty of Art and Sciences, Department of Physics, 55139 Samsun, Turkey
E-mail: bbulut@omu.edu.tr